Domain Walls and Bound States in the One-Dimensional Quantum Ising Model

Diego De Gusem & Ian Lateur*

Academic year 2022-2023

Abstract

The quantum transverse field Ising chain is extensively numerically studied. It has two magnetic fields: the transverse field g which generates disorder, and the longitudinal field h_z which generates order. The magnetisation behaves like the classical 2D Ising system when mapping g to temperature T and h_z to the magnetic field. It shows critical behaviour at $g = 0.5$, where the critical exponent $\beta = 1/8$ is found for the magnetisation. The theoretical dispersion relations for the first excitation for various g at $h_z = 0$ is also correctly found. When adding a small longitudinal field $0 < h_z \ll 1$, the ratio E_2/E_1 of the second and first excitation energies approaches the golden ratio when approaching criticality. This is because of the E_8 symmetry the system attains. The other six excitations lie within the energy continuum and are untraceable with the method used. When adding this small field h_z to any $g < 0.5$, the excitations become bound kink anti-kink states. The energy of these states is predicted reasonably well by solving the single particle Schrödinger equation for a linear potential well. It still holds when adding small momentum k.

*with lots of guidance from Lukas Devos

Contents

1 Introduction

In this project, the infinite one dimensional quantum Ising model will be studied numerically[1] using tensor network techniques. The heavy lifting is done with MPSKit [6] in the Julia programming language [1]. The thermodynamic limit $N = \infty$ is no problem for matrix product states, as translational invariance can be exploited. The following Ising chain Hamiltonian is used, as found in MPSKitModels [7].

$$\hat{H} = -J \sum_i \left(\hat{S}_i^z \hat{S}_{i+1}^z + g \hat{S}_i^x + h_z \hat{S}_i^z \right) \tag{1}$$

Operators $\hat{S}_i^z$ and $\hat{S}_i^x$ act on lattice site i and are $\frac{1}{2}$ times the Pauli matrices σ^z and σ^x. This is different from the Hamiltonian used in the syllabus Strongly Correlated Quantum Systems [4].

$$\tilde{H} = -\tilde{J} \sum_{\langle i,j \rangle} \sigma_i^z \sigma_j^z - \tilde{h}_x \sum_i \sigma_i^x - \tilde{h}_z \sum_i \sigma_i^z \tag{2}$$

$$= -\tilde{J} \sum_i \left(\sigma_i^z \sigma_{i+1}^z + \tilde{g} \sigma_i^x + \frac{\tilde{h}_z}{\tilde{J}} \sigma_i^x \right) \tag{3}$$

The coefficients can be converted into each other.

$$\tilde{J} = \frac{J}{4} \qquad \tilde{g} = 2g \qquad \tilde{h}_z = \frac{1}{2} h_z J \tag{4}$$

The quantum Ising chain with $h_z = 0$ has two phases: the symmetry broken phase, $g < 0.5$, with two distinct ground states ($|\uparrow\uparrow\uparrow \ldots \uparrow\rangle$ or $|\downarrow\downarrow\downarrow \ldots \downarrow\rangle$) and the symmetric phase with $g > 0.5$ ($|\rightarrow\rightarrow\rightarrow \cdots \rightarrow\rangle$).

The first excitation can be calculated theoretically, giving the following dispersion relation, with momentum k [4].

$$\epsilon(k) = \frac{J}{2} \sqrt{(\cos(k) - 2g)^2 + \sin^2(k)} \tag{5}$$

For $g < 0.5$ this can be seen as a single domain wall between semi-infinite up and semi-infinite down domains ($|\ldots\uparrow\uparrow\underline{|\downarrow\downarrow}\ldots\rangle$). For $g > 0.5$ this is a single left facing spin in between infinite right facing spins ($|\cdots\rightarrow\rightarrow\leftarrow\rightarrow\rightarrow\ldots\rangle$). Excitations can be calculated numerically with the "quasi particle ansatz".

For the remainder of this text, J will be set to 1, unless stated otherwise. This is equivalent to using J as the energy unit.

2 Exploring the Ground State

In this section, the behaviour of the ground state will be explored for different combinations of parameters h_z and g. An appropriate bond dimension should be chosen. For this purpose a

[1]The code for all the figures can be found here: https://github.com/Riculo1/SCQS_Ising

plot of the entanglement entropy as a function of the bond dimension was made at the critical value $g = 0.5$, as this is the most difficult to calculate, and can be seen in figure 1. With this figure a bond dimension of 20 is chosen, as the entanglement entropy is already down to 10^{-3}.

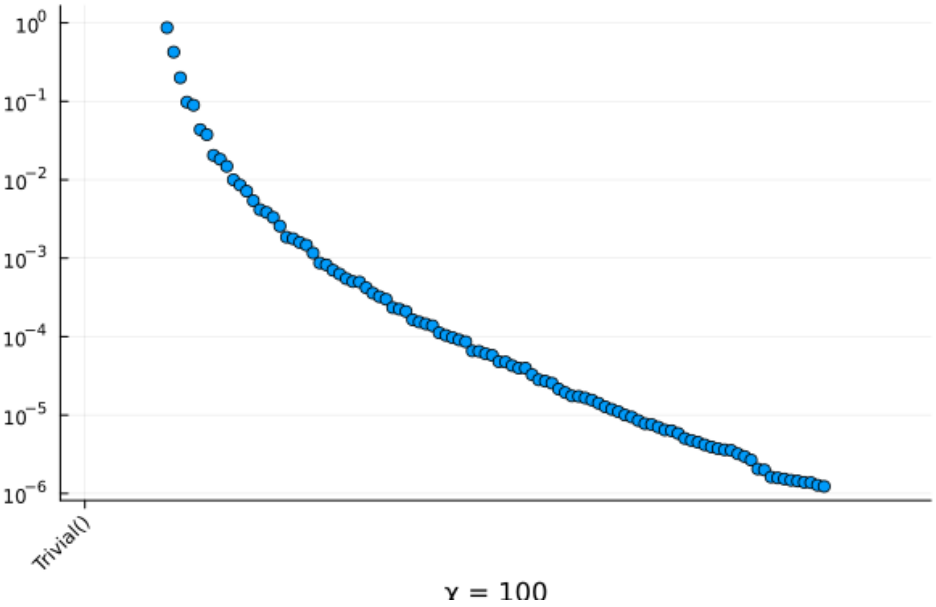

Figure 1: The entanglement entropy as a function of the bond dimension for $g = 0.5$ and $h_z = 0$.

Some magnetisation curves are made for different values of h_z, see figure 2. In this plot it can already be confirmed that $g = 0.5$ is in fact the critical point for $h_z = 0$. This is also completely analogous to the classical 2D Ising model where g is the temperature and h_z an external magnetic field. This can also be confirmed in figure 3, which is a heatmap of the magnetisation as a function of g and h_z. In the classical 2D Ising model the magnetisation curve for no external field becomes a power law with a critical exponent β when taking the lower limit of temperature T towards the critical value T_c when no external field is applied. In this case the magnetisation is proportional to $\left(\frac{T_c - T}{T_c}\right)^{\beta}$ [2], which can easily be written in terms of g for the transverse field Ising model.

$$m \sim \left(\frac{g_c - g}{g_c}\right)^{\beta} \tag{6}$$

A fit of this equation on a magnetisation curve can be found in figure 4a. In theory the value of β should be 1/8 [2], the fit gave a value of 0.123. Another interesting thing to look at is the value of β in function of the bond dimension, this can be seen in figure 4b. On this figure it is clear that the computed value approaches the real value when the bond dimension increases.

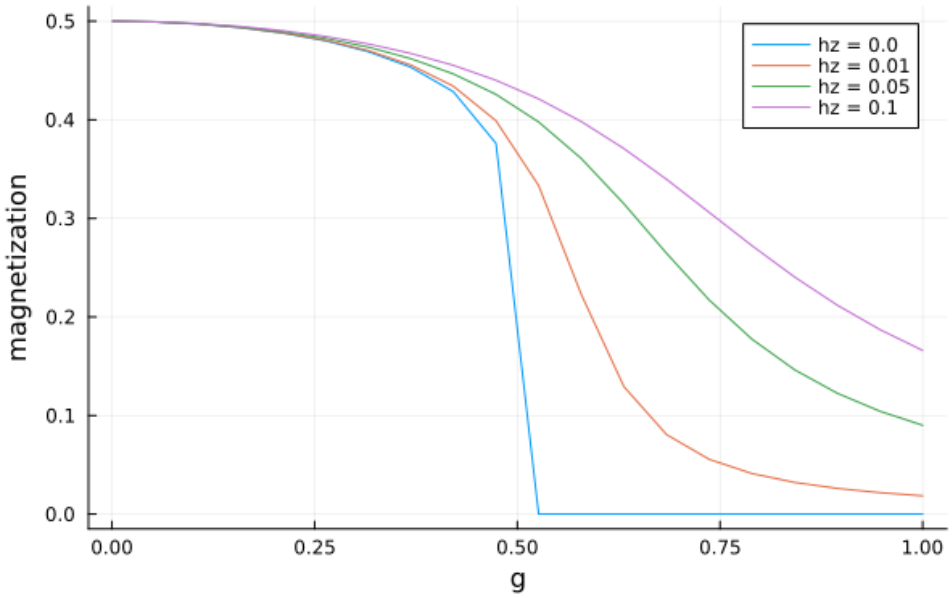

Figure 2: Magnetisation in function of g for different values of hz.

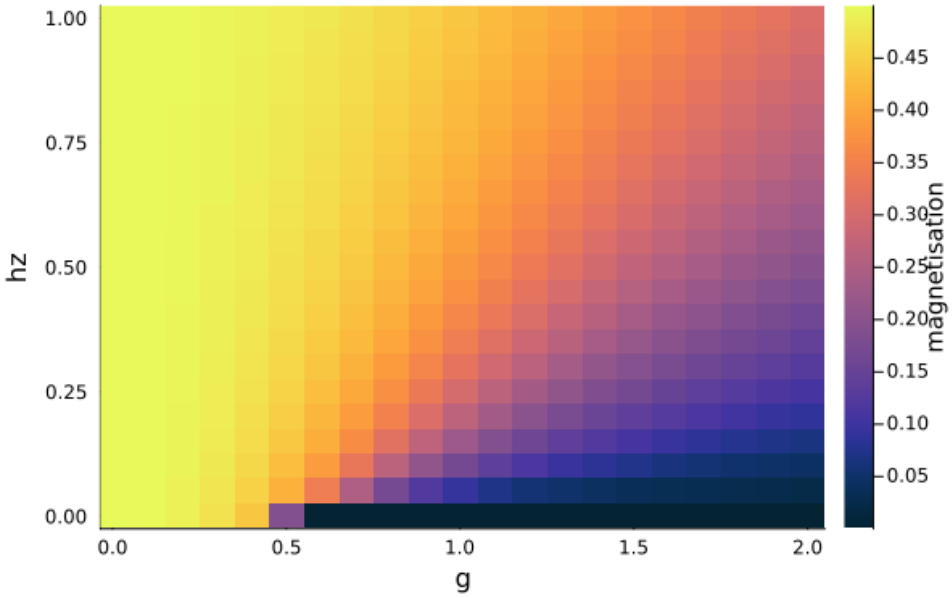

Figure 3: The absolute value of the magnetisation for different values of g and h_z.

3 Comparing Dispersion Relations

To check the validity of equation (5) for the first excited state, the bond dimension has to be chosen correctly. This has been done in figure 5. This is the difference between theoretical and numerical first excitation energy at critical value $g = 0.5$ and momentum $k = 0$ as a function of virtual bond dimension D. It is expected that the critical value is the most difficult to simulate, so if this one is converged to the required accuracy, the other ones will likely be too. It can be seen that bond dimension $D = 20$ yields an accuracy of $0.001J$.

The first attempt to show the validity of the equation can be seen in figure 6. A ground state is created and the first excitation is calculated on top. This method is successful for

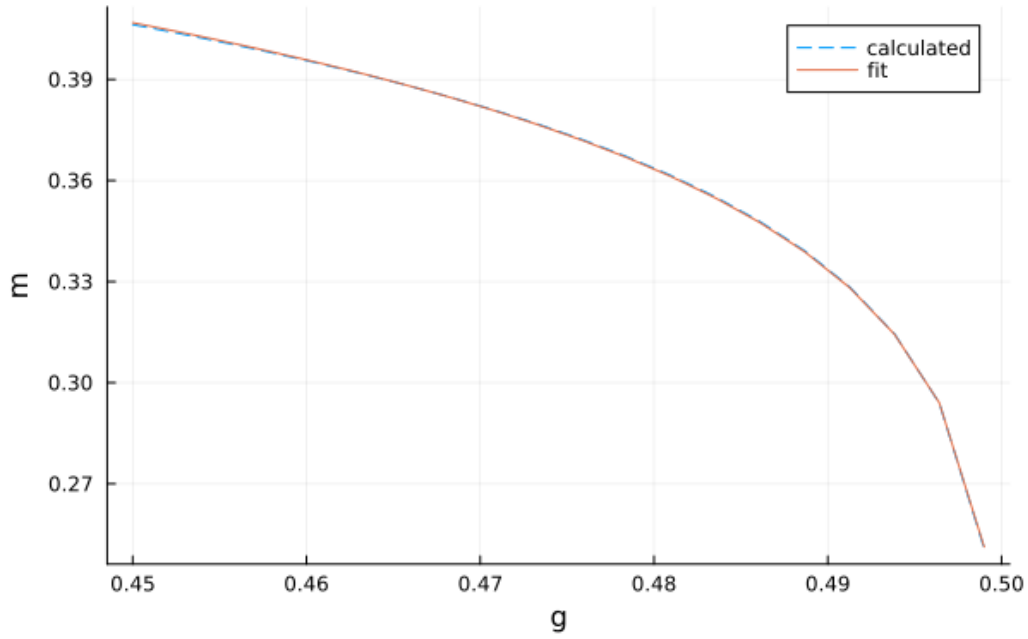

(a) Fit of the critical exponent for $D = 25$. The blue dotted line is the numerically calculated curve and the red line is a fit.

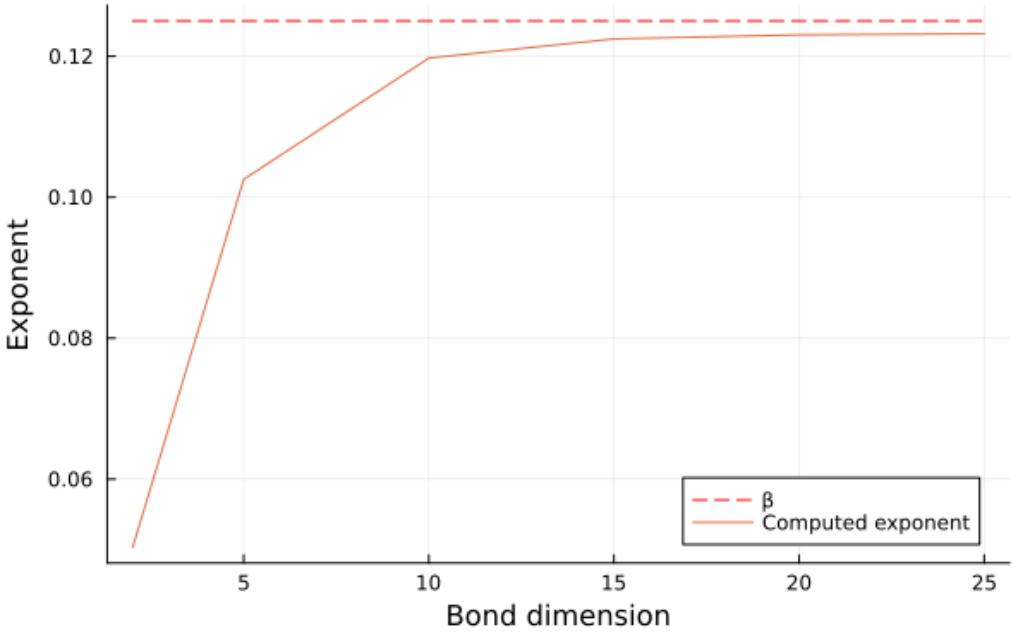

(b) Critical exponent in function of the bond dimension.

Figure 4: Fit of the critical exponent β in $m \sim \left(\frac{g_c - g}{g_c}\right)^{\beta}$ for the magnetisation curve and comparison with the real value of 1/8. The exponent is found to be 0.123 when $D = 25$.

$g \geq 0.5$, but fails for $g < 0.5$. This is because both boundaries stay in the up direction, so the first excitation found is not $|\ldots \uparrow\uparrow \underline{\downarrow\downarrow} \ldots\rangle$ but $|\ldots \uparrow\uparrow \underline{\downarrow} \uparrow\uparrow \ldots\rangle$, which is actually the second excitation. This is no problem for $g \geq 0.5$, because this needs exactly one flip.

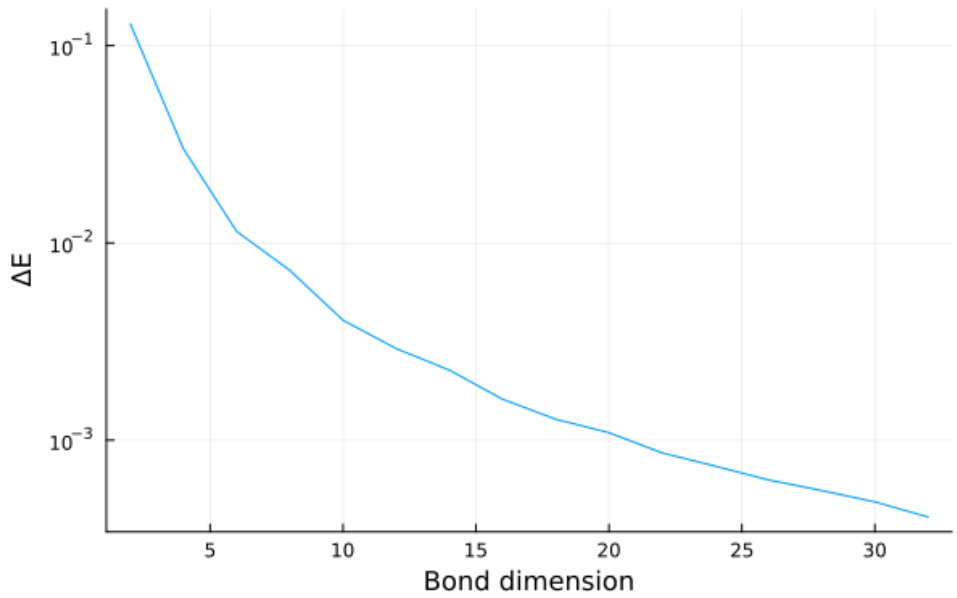

Figure 5: The difference between theoretical and numerical first excitation energy at critical value $g = 0.5$ and momentum $k = 0$ as a function of virtual bond dimension D.

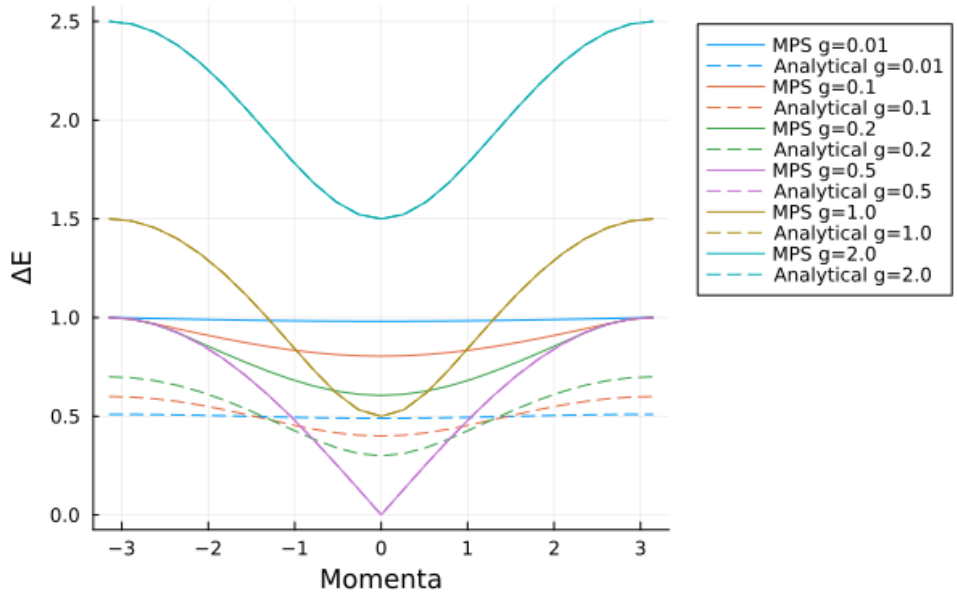

Figure 6: First attempt to calculate dispersion relations of the first excited state for various values of g. For the symmetry broken phase, $g < 0.5$, the numerical result is twice the theoretical prediction.

To solve this problem it is necessary to generate two ground states: one entirely up and one down and connect these two. In figure 7 it can be seen that this indeed solves the problem and shows perfect compatibility with the theoretical dispersion relation.

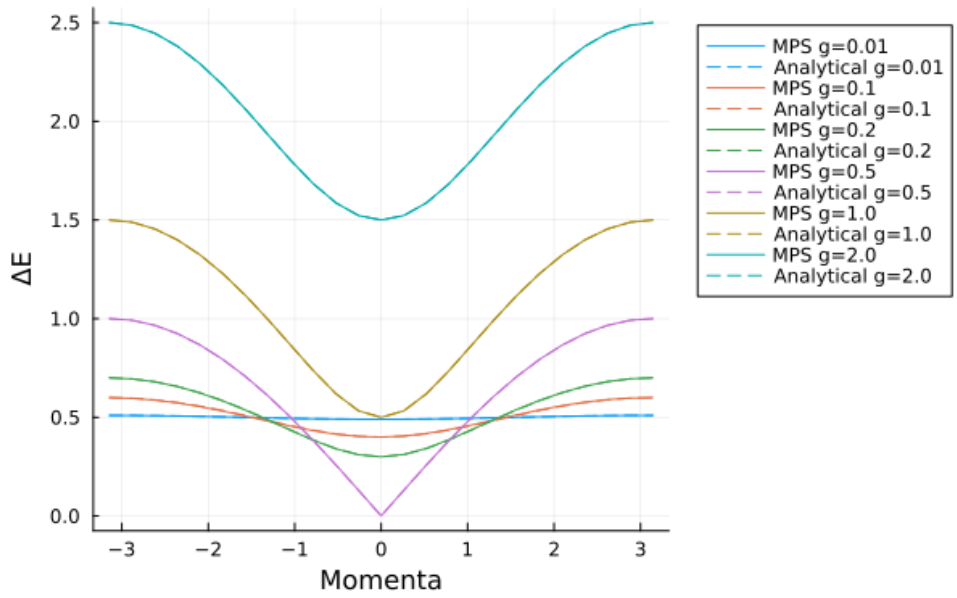

Figure 7: Correctly calculated dispersion relations of the first excited state for various values of g.

4 The Golden Ratio

4.1 Converging

It is said that the ratio of the masses of the two first excited states, m_2/m_1, or equivalently the ratio of the energies of the first two excited states, E_2/E_1, approaches the golden ratio when g approaches the critical value from below and h_z is small [3] [5]. Masses and energies will be used interchangeably.

In order to reproduce this result, an appropriate bond dimension should be chosen. For this, different "small" values of h_z are selected and the energies of the first two excited states are calculated. The ratio E_2/E_1 is compared with the golden ratio, Φ as a function of the bond dimension, see figure 8.

It is already clear that larger values for h_z converge more quickly, meaning they are easier to simulate. However, smaller h_z converge better to the golden ratio, because the theoretical requirement of "small h_z" is better met.

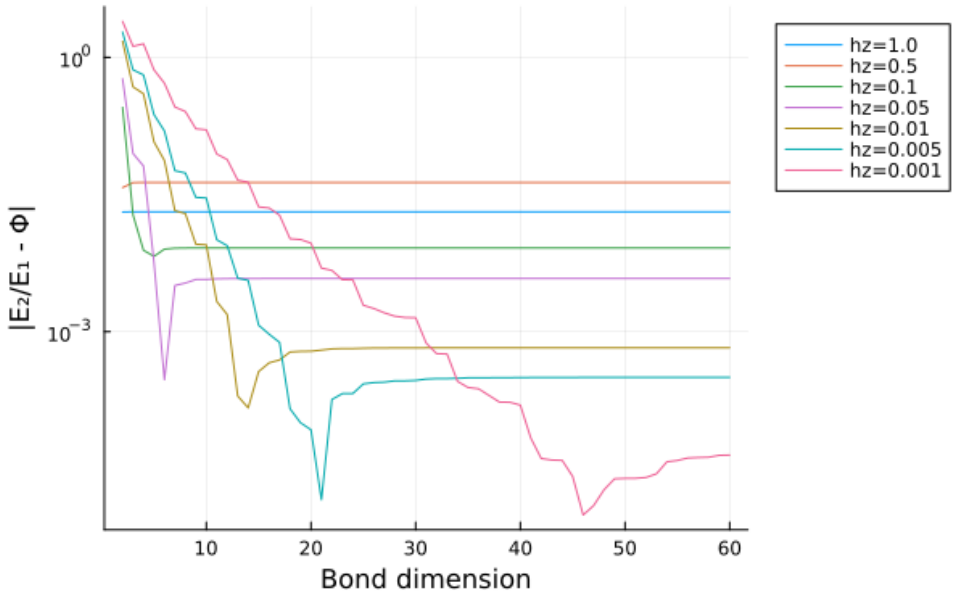

Figure 8: The difference between the golden ratio, $\Phi = \frac{1+\sqrt{5}}{2}$, and the energy ratio of the first excited state, E_1, and the second excited state, E_2, in function of the bond dimension, D, at $g = 0.5$ for different values of h_z.

At bond dimension $D = 60$ all energies are converged. With this bond dimension a new figure can be made, figure 9, where the ratio E_2/E_1 is seen as a function of g. It can again be seen that if h_z is too big (1.0 and 0.5 on the figure), the ratio does not converge to the golden ratio and when h_z gets smaller, the curves do approach the golden ratio. The closest value achieved with these parameters is around ~ 1.61799 at $g = 0.5$ and $h_z = 0.001$, which differs 0.003% from the golden ratio. To get an even better result h_z could be made even smaller, but then the bond dimension should be made larger.

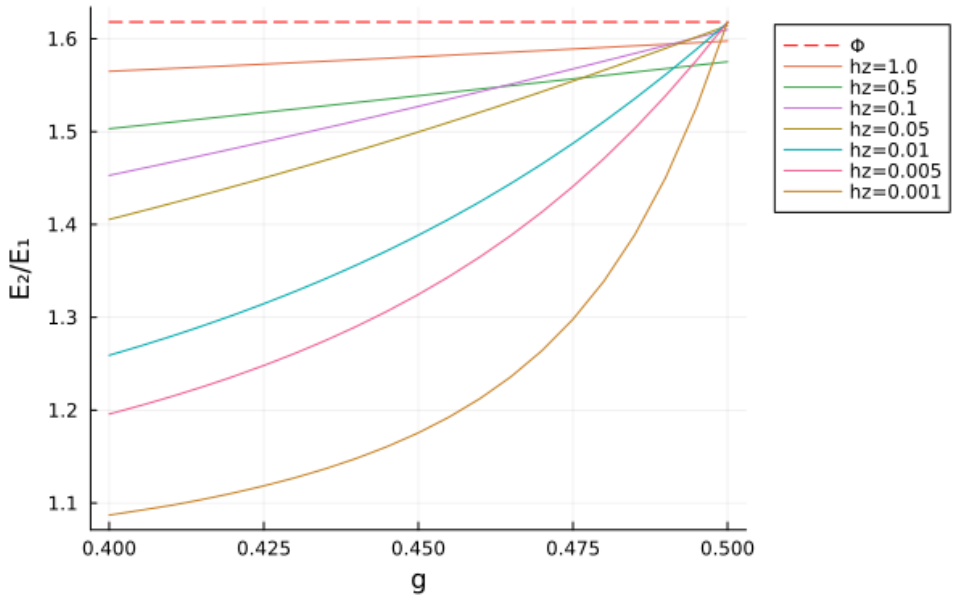

Figure 9: The ratio of the energy of the first excited state, E_1, and the second excited state, E_2, in function of g for different h_z and with bond dimension 60. It can be seen that at $g = 0.5$ and small h_z, the curves approach the golden ratio $\Phi = \frac{1+\sqrt{5}}{2}$.

4.2 More Excitations and the E_8 Lie Group

Theoretically, the one-dimensional quantum Ising system gains the E_8 symmetry near criticality [5]. The E_8 Lie group has a spectrum of 8 particles. These were first described in the context of mesons, but work perfectly as excitations too. The first particle has some mass (or energy) m_1. The others have the following masses [3]:

$$\begin{aligned}
m_2 &= 2m_1 \cos\frac{1}{5}\pi &&= (1.6180339887\ldots)m_1,\\
m_3 &= 2m_1 \cos\frac{1}{30}\pi &&= (1.9890437907\ldots)m_1,\\
m_4 &= 2m_2 \cos\frac{7}{30}\pi &&= (2.4048671724\ldots)m_1,\\
m_5 &= 2m_2 \cos\frac{2}{15}\pi &&= (2.9562952015\ldots)m_1,\\
m_6 &= 2m_2 \cos\frac{1}{30}\pi &&= (3.2183404585\ldots)m_1,\\
m_7 &= 4m_2 \cos\frac{1}{5}\pi\cos\frac{7}{30}\pi &&= (3.8911568233\ldots)m_1,\\
m_8 &= 4m_2 \cos\frac{1}{5}\pi\cos\frac{2}{15}\pi &&= (4.7833861168\ldots)m_1.
\end{aligned}$$

In principle, all eight should exist within this system. However, m_3 to m_8 are numerically untraceable (at least with the quasi particle ansatz), as there is a continuum of energies at and above $2m_1$. At that point, there is enough energy to create two m_1 particles with opposing, but continuous, momenta.

5 Spectrum of Bound Kink Anti-Kink States

5.1 Theoretical Discussion

The first excitation in the symmetry broken phase ($g < \frac{1}{2}$, $h_z = 0$) is a single domain wall, or kink, between two semi-infinite domains: $\big|\ldots\overline{\uparrow\uparrow}\big|\underline{\downarrow\downarrow}\ldots\big\rangle$. However, when a non-zero, but small longitudinal field is added, $0 < h_z \ll 1$, the $\mathbb{Z}_2$ symmetry is explicitly broken. The down $\downarrow$ configuration is slightly less favourable than the up $\uparrow$ configuration, meaning a semi-infinite domain of down spins becomes impossible. At some point an anti-kink will need to be made: $\big|\ldots\overline{\uparrow\uparrow}\big|\underline{\downarrow\ldots\downarrow}\big|\overline{\uparrow\uparrow}\ldots\big\rangle$. This effectively binds kink and anti-kink 'particles' with a linear potential energy $V(x) = \lambda|x|$ with kink separation x. The 'string tension' λ is equal to Jh_z as can be seen by studying the Hamiltonian (1). This holds as long as it remains 'cheaper' to extend the length of the down domain than to create a new boundary or kink anti-kink pair.

As described in [5], the essential physics of confinement is apparent in the limit of small λ ($h_z \ll 1$) for two kinks near the band minimum ($k \ll 1$), where the one-kink dispersion (5) is

quadratic.

$$\epsilon(k) = m_0 + \frac{\hbar^2 k^2}{2\mu} + \mathcal{O}(x^4) \tag{7}$$

$$= \frac{J}{2}(1-2g) + \frac{Jg}{2(1-2g)}k^2 + \mathcal{O}(x^4) \tag{8}$$

The one-kink creation energy is $m_0 = \frac{J}{2}(1-2g)$ and the effective mass is $\frac{\mu}{\hbar^2} = \frac{1-2g}{Jg}$. The Schrödinger equation for the relative motion of the two kinks in their centre-of-mass frame is

$$-\frac{\hbar^2}{\mu}\frac{\mathrm{d}^2\phi}{\mathrm{d}x^2} + (2m_0 + \lambda|x|)\phi = m\phi, \tag{9}$$

which has only bound state solutions with energies or masses

$$m_j = 2m_0 + z_j \left(\frac{\lambda^2\hbar^2}{\mu}\right)^{\frac{1}{3}} \tag{10}$$

$$= J(1-2g) + z_j J \left(\frac{h_z^2 g}{1-2g}\right)^{\frac{1}{3}}. \tag{11}$$

The prefactors z_j are the negative zeros of the Airy function $Ai(-z_j) = 0$, which are about 2.34, 4.09, 5.52, 6.79, etc.

Adding small momentum k to the kink anti-kink pair generalizes [5] the energy (10) to

$$m_j(k) = 2\epsilon\left(\frac{k}{2}\right) + z_j \left(\frac{\lambda^2\hbar^2}{\mu}\right)^{\frac{1}{3}} \tag{12}$$

$$= J\sqrt{(\cos(k/2) - 2g)^2 + \sin^2(k/2)} + z_j J \left(\frac{h_z^2 g}{1-2g}\right)^{\frac{1}{3}}, \tag{13}$$

where the kink and anti-kink each get half of the momentum (5).

5.2 Numerical Search

5.2.1 Finding Bond Dimension D

Like always an appropriate bond dimension should be chosen. In order to do this figure 10 is created for small $g = 0.05$ and small $h_z = 0.01$. From this figure, bond dimension 40 is chosen, as it seems both converged and relatively stable. Lower bond dimensions seem to have a higher chance of failing, which can be seen in the figure as a dip. Running this again yields dips in different places.

5.2.2 Exploring the Parameter Space for Zero Momentum

The relative error of the excitation energy with (10) is plotted as a function of parameters g and h_z for 5 excitations, see figure 11. To get a better overview of where this approximation

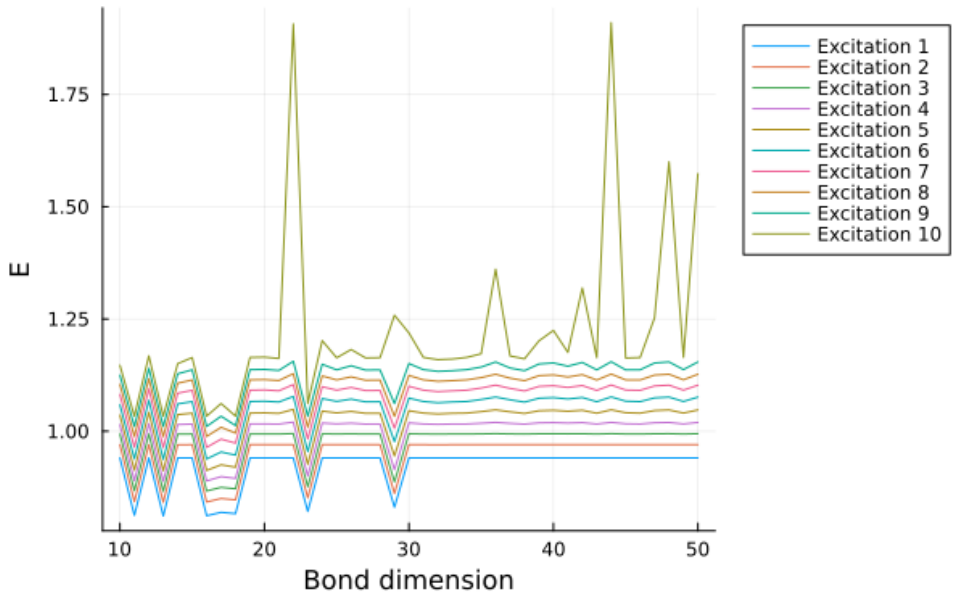

Figure 10: Energy as a function of the bond dimension for excitations one to ten with $g = 0.05$ and $hz = 0.01$ at momentum 0.

is valid, the relative error is cut off at 10% (yellow). The uncolored (white) areas are points where the energy of the excitation is the same as the previous excitation, which means the energy continuum has been reached. Now the maximum relative error of every excitation can be taken at every point to generate a new heatmap. On this figure it is possible to take a point where all of the excitations more or less follow equation (10).

All figures show two distinct parameter regions where the theoretical approximation (10) is valid. The first region is at very low h_z for almost all g, except close to critial value 0.5. The second region is a diagonal line, which varies from excitation to excitation. For the first region figure 12 is created. On this image there is some noise for very low h_z, not because the models necessarily fails, but because the bond dimension should be higher for those values.

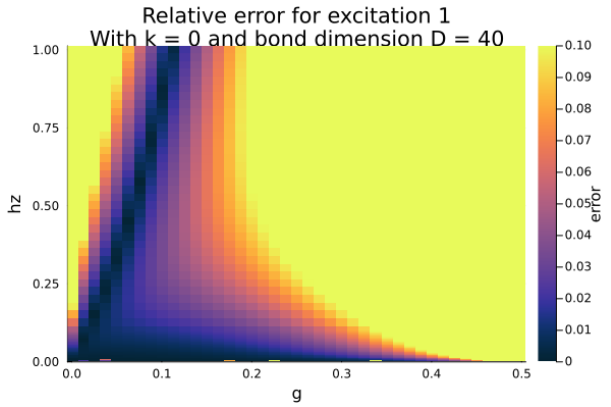

(a) Excitation 1.

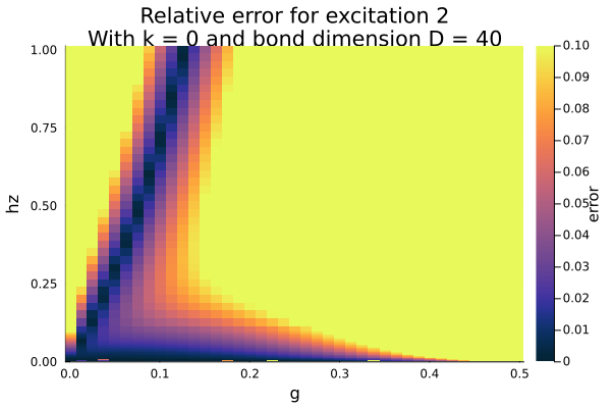

(b) Excitation 2.

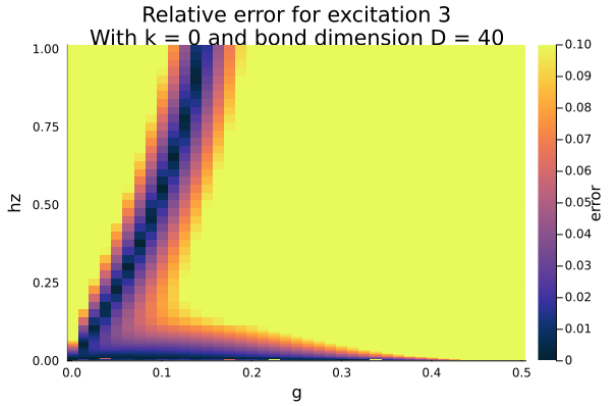

(c) Excitation 3.

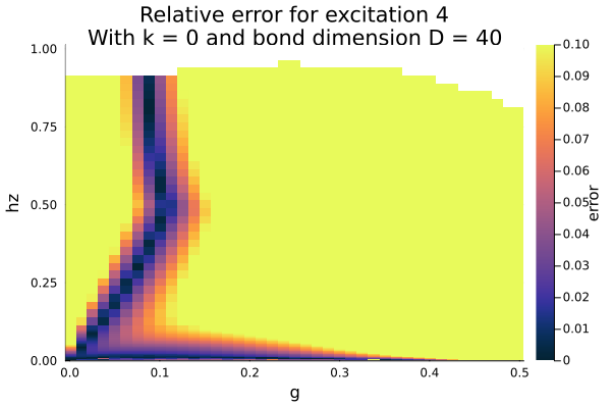

(d) Excitation 4.

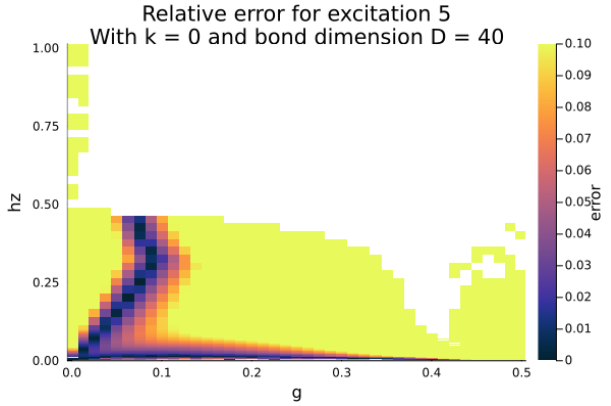

(e) Excitation 5.

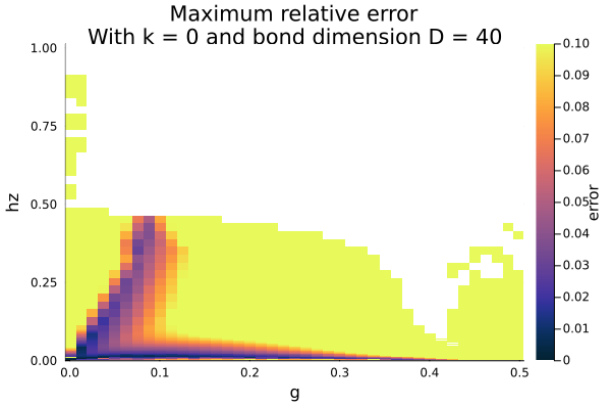

(f) Maximum relative error.

Figure 11: Heatmaps of the relative error between the theoretical excitation energy using the Airy function and the calculated excitation energy for excitations one to five. These have been made for momentum 0 and bond dimension 40 for g going from 0.001 to 0.499 and h_z going from 0.0002 to 1.

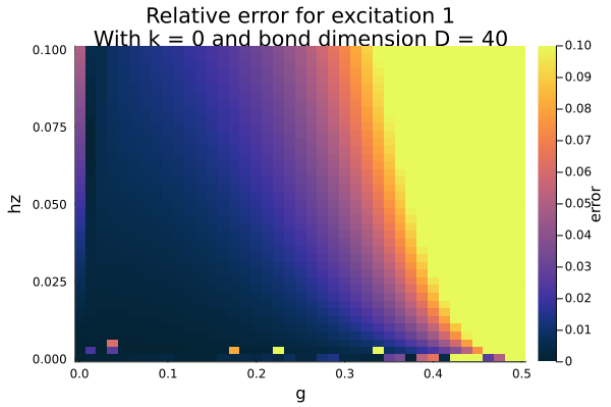

(a) Excitation 1.

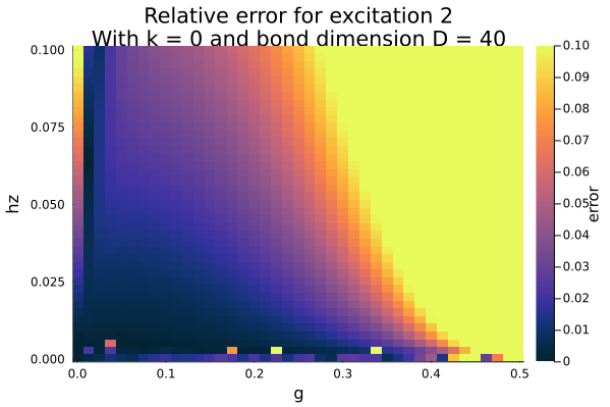

(b) Excitation 2.

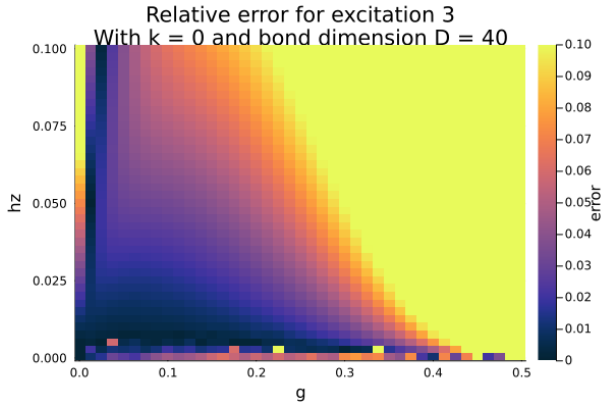

(c) Excitation 3.

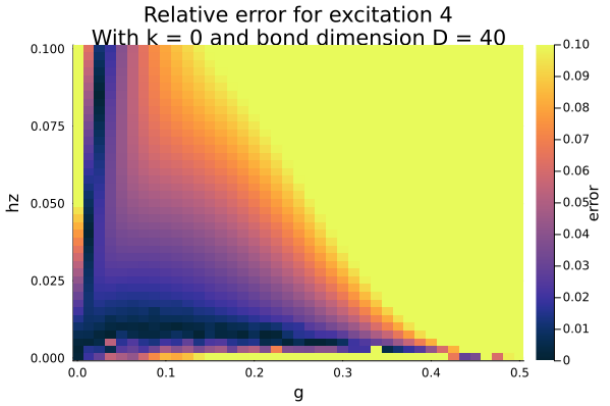

(d) Excitation 4.

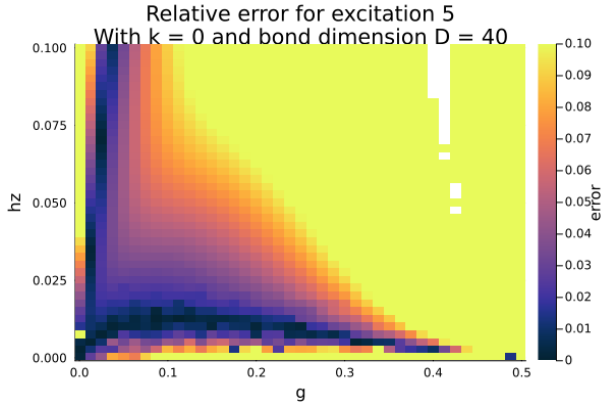

(e) Excitation 5.

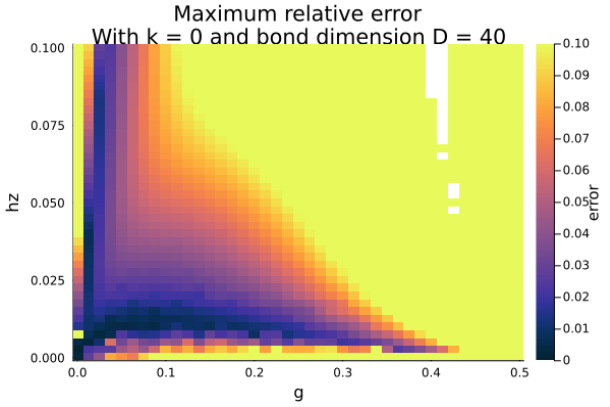

(f) Maximum relative error.

Figure 12: Heatmaps of the relative error between the theoretical excitation energy using the Airy function and the calculated excitation energy for excitations one to five. These have been made for momentum 0 and bond dimension 40 for g going from 0.001 to 0.499 and h_z going from 0.0002 to 0.1.

5.2.3 Adding Momentum

For both regions a point is chosen somewhat in the middle which has a low maximum relative error. For the low h_z region $g = 0.2$ and $h_z = 0.0075$ is chosen, which has an error of 0.8% for $k = 0$. For the diagonal line region $g = 0.075$ and $h_z = 0.35$ is chosen, which has an error of 3%. At both points momentum is added. The resulting energies are compared to equation (12), which can be seen in figure 13 and 14 respectively.

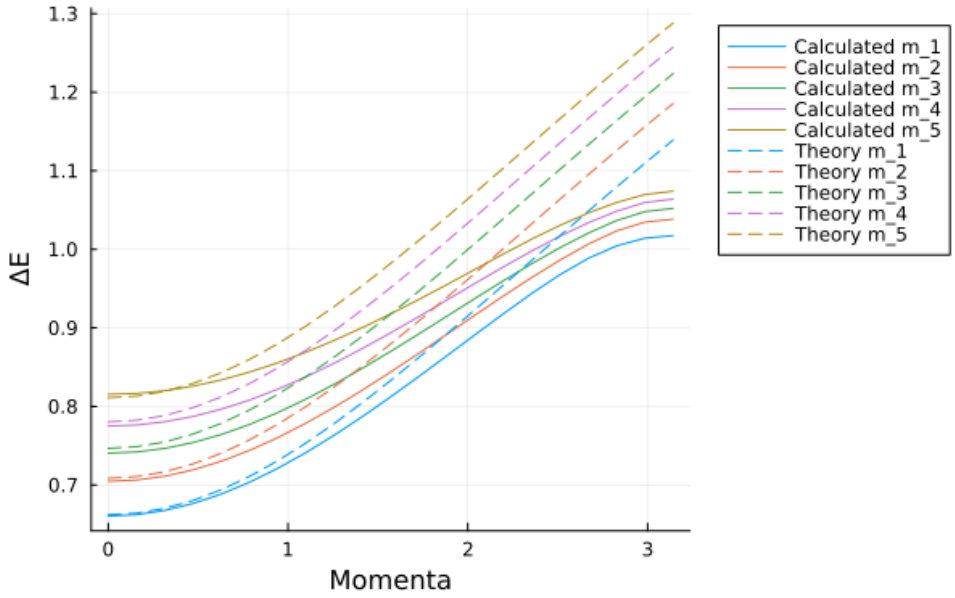

Figure 13: Dispersion relation for $g = 0.2$ and $h_z = 0.0075$ compared with equation 12. At momentum 0 the calculated energy gave an error of 0.8% on figure 11. This is clearly not an accident.

The theoretical prediction follows the obtained energies pretty closely for low momentum for the first point. The lower excitations are better predicted than the higher ones. On the other hand, the second point only seems to be accidentally close to the theoretical result (10), but the energy-momentum behaviour is not the same. It would seem that the diagonal lines, which vary from excitation to excitation, are close to the prediction by chance, while the low h_z region is actually correctly predicted. This is precisely the parameter region for which equations (10) and (12) were engineered (low h_z, low k).

5.2.4 Checking h_z Scaling

Lastly the excitation energy should follow $h_z^{\frac{2}{3}}$ according to equation (10). The energy is firstly plotted as a function of bond dimension D for low $h_z = 0.0025$ in figure 15, as lower h_z seemed to require the highest bond dimension. With a stable $D = 100$ the magnetic field h_z is varied within the previously purple region $h_z \in [0, 0.01]$ for a constant $g = 0.0125$. The lowest excitation energies follow the predicted mass well, but the model seems to break sooner for higher excitations. While in theory this may be $h_z^{\frac{2}{3}}$, it may as well be a linear relation. If even lower h_z want to be simulated, the bond dimension needs to be increased even higher.

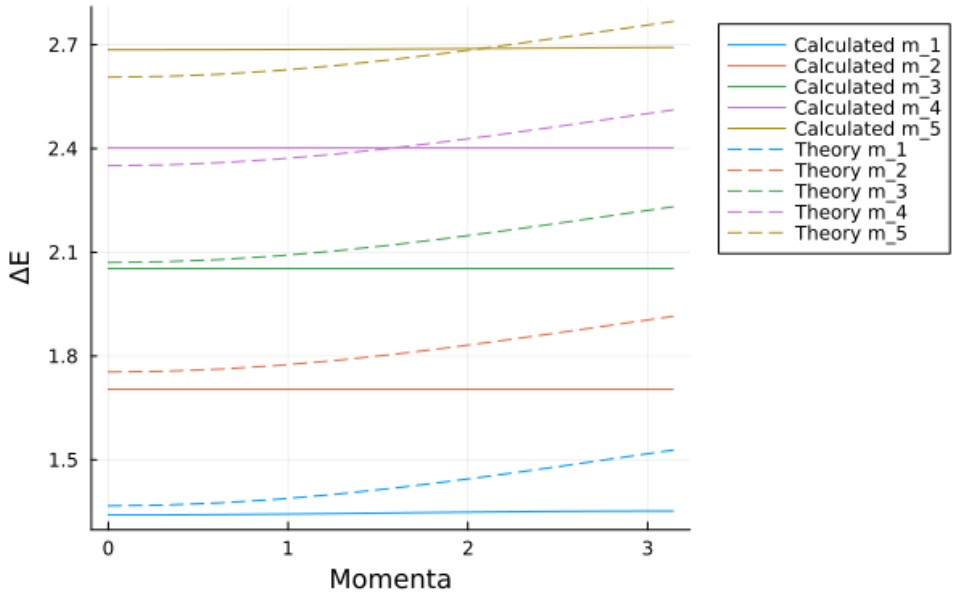

Figure 14: Dispersion relation for $g = 0.075$ and $h_z = 0.35$ compared with equation 12. At momentum 0 the calculated energy gave a maximum error of 3% on figure 11. This seems to be accidental.

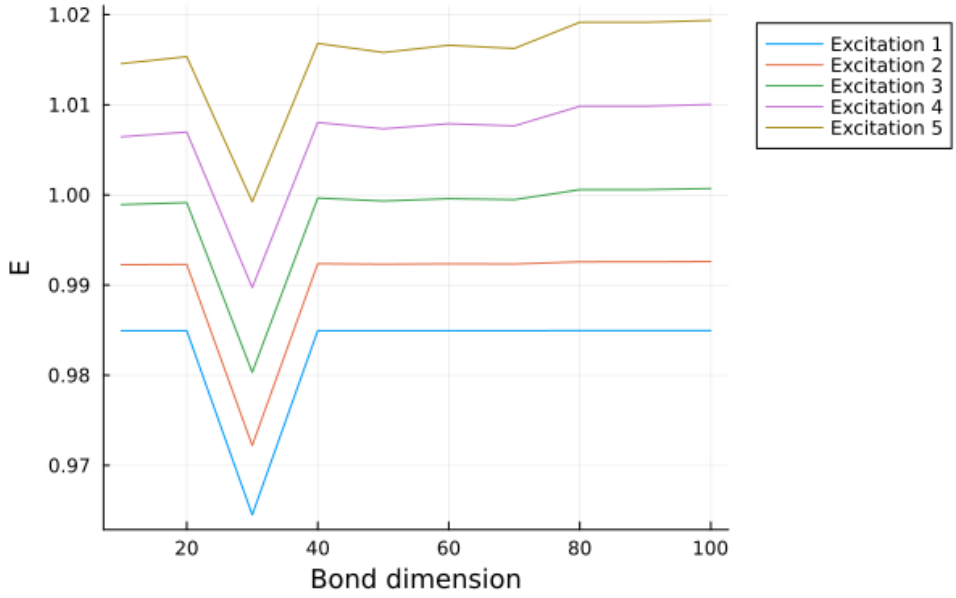

Figure 15: Energy as a function of bond dimension for $g = 0.0125$ and $h_z = 0.0025$ with momentum 0.

6 Conclusion

The quantum transverse field Ising chain has been extensively numerically studied. The magnetisation behaves like the classical 2D Ising system when mapping g to temperature T and h_z to the magnetic field. It shows critical behaviour at $g = 0.5$, where the critical exponent $\beta = 1/8$ is found for the magnetisation. The theoretical dispersion relations for the first excitation for various g at $h_z = 0$ is also correctly found. This required a little engineering, because for $g < 0.5$ the left and right semi-infinite domains are different, as the excitation is only a

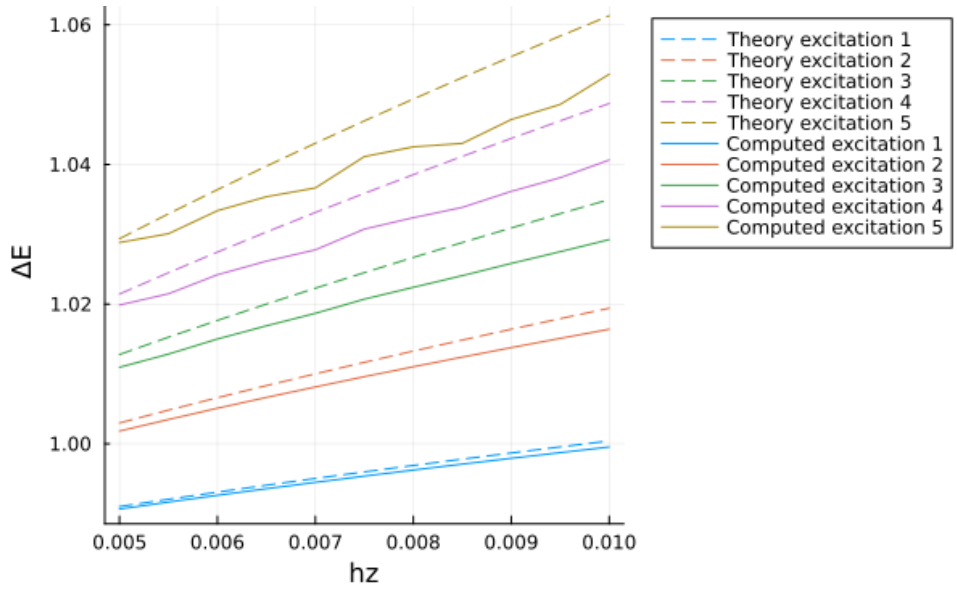

Figure 16: Energy as a function of h_z compared with the theoretical function for $g = 0.0025$, $D = 100$.

single domain wall. When adding a small longitudinal field $0 < h_z \ll 1$, the ratio E_2/E_1 of the second and first excitation energies approaches the golden ratio when approaching criticality. The other six excitations lie within the energy continuum and are untraceable with the method used. The energies of bound kink anti-kink states for $0 < h_z \ll 1$ and $g \in [0, 0.5)$ are predicted reasonably well by solving the single particle Schrödinger equation for a linear potential well. The smaller h_z is, the better the prediction holds, but the more difficult the simulation becomes and thus the higher the bond dimension D needs to be. The prediction still holds when adding small momentum k. In general lower excitations are predicted better than higher ones.

References

[1] Bezanson, J., Edelman, A., Karpinski, S., & Shah, V. B. (2017). *Julia: A fresh approach to numerical computing*. SIAM Review, 59(1), 65–98. DOI: https://doi.org/10.1137/141000671.

[2] E. Ibarra-García-Padilla et al. 2016. "The Hobbyhorse of Magnetic Systems: The Ising Model". *Eur. J. Phys.* **37** 065103. DOI: https://doi.org/10.1088/0143-0807/37/6/065103.

[3] G. Delfino and G. Mussardo. "The spin-spin correlation function in the two-dimensional Ising model in a magnetic field at T= Tc". In: *Nuclear Physics B* 455.3 (1995), pp. 724–758. DOI: https://doi.org/10.1016/0550-3213(95)00464-4.

[4] Haegeman, J., Vanderstraeten, L. (2023). *Strongly Correlated Quantum Systems* [Syllabus]. Quantum Group, Ghent University.

[5] R. Coldea et al. (2010). Quantum Criticality in an Ising Chain: Experimental Evidence for Emergent E8 Symmetry. *Science*, *327*(5962), 177-180. DOI: https://doi.org/10.1126/science.1180085.

[6] Van Damme, M., et al. (2023). *MPSKit.jl: Includes code for tackling 1 dimensional (quantum) problems using tensor network algorithms*. Retrieved from GitHub Repository https://github.com/maartenvd/MPSKit.jl.

[7] Van Damme, M., et al. (2023). *MPSKitModels.jl*. Retrieved from GitHub Repository https://github.com/maartenvd/MPSKitModels.jl.